Anal Bioanal Chem (2006) 386: 444–457
DOI 10.1007/s00216-006-0541-z

REVIEW

Wei Du · Ying Wang · Qingming Luo · Bi-Feng Liu

Optical molecular imaging for systems biology: from molecule to organism

Received: 31 January 2006 / Revised: 1 May 2006 / Accepted: 9 May 2006 / Published online: 19 July 2006

Abstract The development of highly efficient analytical methods capable of probing biological systems at system level is an important task that is required in order to meet the requirements of the emerging field of systems biology. Optical molecular imaging (OMI) is a very powerful tool for studying the temporal and spatial dynamics of specific biomolecules and their interactions in real time in vivo. In this article, recent advances in OMI are reviewed extensively, such as the development of molecular probes that make imaging brighter, more stable and more informative (e.g., FPs and semiconductor nanocrystals, also referred to as quantum dots), the development of imaging approaches that provide higher resolution and greater tissue penetration, and applications for measuring biological events from molecule to organism level, including gene expression, protein and subcellular compartment localization, protein activation and interaction, and low-mass molecule dynamics. These advances are of great significance in the field of biological science and could also be applied to disease diagnosis and pharmaceutical screening. Further developments in OMI for systems biology are also proposed.

Keywords Optical molecular imaging · Fluorescent protein · Quantum dots · Systems biology · Review

Abbreviations AFP: *Aequorea* fluorescent protein · CFP: Cyan fluorescent protein · cpGFP: Circularly permuted green fluorescent protein · cpYFP: Circularly permuted yellow fluorescent protein · EGFP: Enhanced green fluorescent protein · EYFP: Enhanced yellow fluorescent protein · FCS: Fluorescence correlation spectroscopy · FISH: Fluorescence in situ hybridization · FLIM: Fluorescence lifetime imaging microscopy · FP: Fluorescent protein · FRAP: Fluorescence recovery after photobleaching · FRET: Fluorescence resonance energy transfer · FSM: Fluorescent speckle microscopy · GFP: Green fluorescent protein · LSCM: Laser scanning confocal microscopy · MPLSM: Multiple-photon laser scanning microscopy · OMI: Optical molecular imaging · QDs: Quantum dots · RS: Raman spectroscopy · ROI: Regions of interest · SBT: Spectral bleed-through · WFM: Wide-field microscopy · YFP: Yellow fluorescent protein

W. Du · Y. Wang · Q. Luo · B.-F. Liu (✉)
The Key Laboratory of Biomedical Photonics of MOE—Hubei Bioinformatics & Molecular Imaging Key Laboratory,
Department of Systems Biology,
College of Life Science and Technology,
Huazhong University of Science and Technology,
Wuhan 430074, People's Republic of China
e-mail: bfliu@mail.hust.edu.cn
Tel.: +86-27-87792203
Fax: +86-27-87792203

Bi-Feng Liu
is Professor at Huazhong University of Science and Technology, and serving as Chair of the Department of Systems Biology. His research interest focuses on systems biology-oriented analytical science in the area of micro-separation, nano/microfluidics and optical molecular imaging.

Introduction

Due to the rapid progress in the field of molecular biology that has occurred over the last century, we have come to see that life involves thousands of genes, proteins, metabolites, etc. However, life is not invoked by simply collecting these together; an integrated system formed from those components is required. It is vital to understand biological systems such as molecular networks, cells, tissues and even the organism itself at the system level. This shift in biological paradigm from reductionism to integration has made the field of systems biology [1–5] a new challenge

that is currently a hot topic. Although attempts to systematically understand biological systems can be dated back to Wiener's time [6], research into systems biology represent the first attempts to achieve this based on detailed knowledge of molecules. It promises to reveal the relationships among elements of systems that may include just a few proteins that together perform a defined task or more complex molecular machines, cells and groups of cells, with the goal of understanding their emergent properties [3].

It is widely agreed that systems biology is a large scientific field that relies greatly on collaborations between disciplines such as the life sciences, information science, system engineering and analytical technology. One of the keys to successful research in this field is considered to be work being done in analytical chemistry [7, 8] to develop innovative analytical methods that meet the needs of systems biology research. For example, capillary electrophoresis has been recognized as being the "gold standard" in genomics for DNA sequencing. Similar "gold standard" methods are available in transcriptomics (DNA microarray), proteomics (multidimensional separation coupling with mass spectrometry) and metabolomics (microseparation coupled with mass spectrometry and nuclear magnetic resonance). However, more of these methods are needed. As well as revealing genes, proteins and metabolites from those *omic* investigations, which relate to the basic structures of systems, it is important to have methods capable of monitoring their localizations, connections, and in particular their dynamics over time under various physiological or pathological conditions.

Optical molecular imaging (OMI) is a versatile technique that can be used to investigate the dynamics of biological events in molecules, cells, tissues and organisms in real time and in vivo (Fig. 1) [9–11]. Compared with other imaging approaches like magnetic resonance imaging and positron emission tomography etc., OMI exhibits the great advantages of high temporal (picosecond) and spatial (submicron) resolutions, high sensitivity (single-molecule level) and minimal invasion, and shows high potential for systems biology. This review highlights recent advances in OMI, focusing especially on the development of fluorescent probes such as fluorescent proteins and semiconductor nanocrystals (also referred to as quantum dots, QDs), OMI instrumentation and approaches (techniques). The application of OMI to studies of localization, conformations and interactions of biomolecules in vivo are also highlighted. In particular, this review describes the application of OMI for tracing the dynamics of single molecules and whole-body living organisms, which strongly suggest that OMI is an informative systems biology method that may be used to uncover biological events at different system levels. The future development of OMI is also predicted.

Advances in fluorescent probes

Aequorea fluorescent protein (AFP)-derived mutants

Labeling of biomolecules with fluorescent probes or other dyes has facilitated in vitro or in vivo studies of biomolecular structures and dynamics, as well as their interactions, which is critical if we are to understand the biomolecular mechanisms of cellular function. However, traditional methods of chemical labeling based on fluorescent dyes are often inadequate for biomolecular labeling, repurification and reintroduction into cells by invasive methods like microinjection. These limitations have spawned efforts to noninvasively and site-specifically label protein in living cells or tissues by using green fluorescent protein (GFP) and its variants. The fluorescent protein presents a relatively small size and a compact,

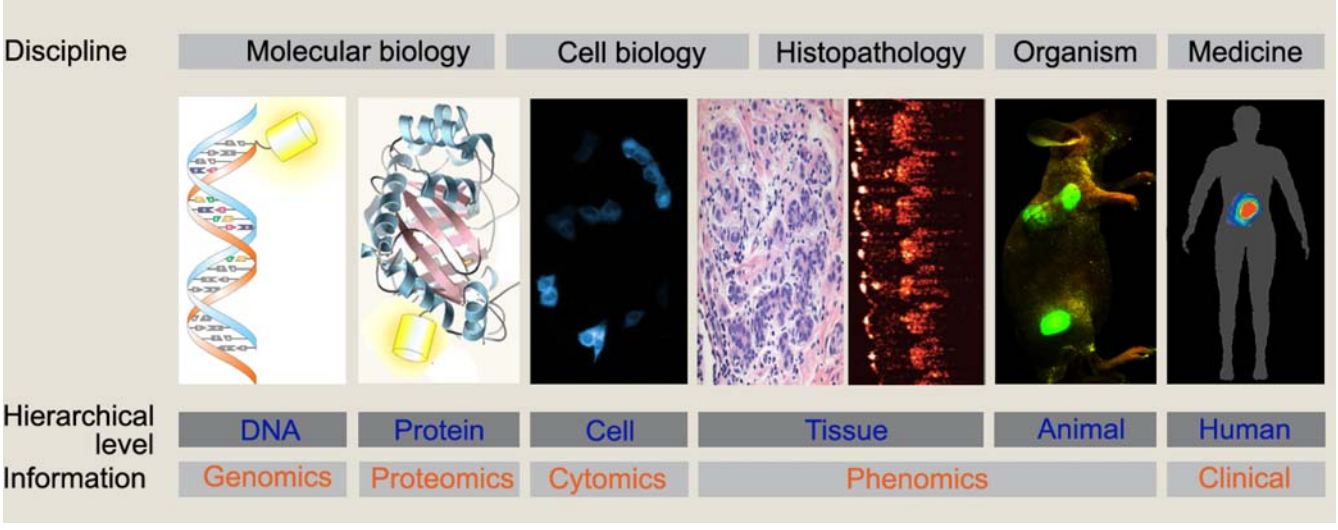

Fig. 1 Utilization of OMI in life science research. OMI can investigate the dynamics of biological events in real time from molecules (*left*), cells, tissues and organisms (*right*) digitally and quantitatively. It can handle a wide range of intensities (about 12 orders of magnitude), times (femtoseconds to years) and spatial dimensions (nanometers to centimeters), and it gives high spatial and temporal resolution of the targeted cellular structures—better than any other method

single-domain structure, which allow it to fuse to other targeted proteins with little or no interference in native protein.

GFP was cloned from *Aequorea victoria*. Excitation of the wild-type GFP by light with a wavelength of 398 nm can induce the emission of bright green fluorescence, peaking at 508 nm. Through continuous efforts to perform protein mutation of GFP, scientists have developed various kinds of AFP with different excitation and emission wavelengths, enhanced brightness, and improved pH resistance compared to the original wide-type, such as enhanced GFP (EGFP), cyan fluorescent protein (CFP) and yellow fluorescent protein (YFP) (Fig. 2a) [12]. The original YFP exhibited several drawbacks when imaging in vivo [13]. Later generations of YFP mutants, including "Citrine" [14] and "Venus" [15], exhibit low pH (5.7) resistance, halide insensitivity, greatly improved photostability, brighter fluorescence, and faster maturation. The original generation of CFP mutants also displayed several spectroscopic disadvantages. By using similar methods to YFP mutagenesis, a CFP mutant named "Cerulean" [16] was obtained, with an improved quantum yield, a higher extinction coefficient and a longer fluorescence lifetime. Another new color GFP mutant, cyan-green fluorescent protein (CGFP) [17], whose excitation and emission wavelengths are intermediate between those of CFP and EGFP, was also found by using this tactic. In addition, "PA-GFP," a GFP mutant, has 100 times greater fluorescence than the original and remains stable for days [18]. These fluorescent proteins were termed molecular or optical highlighters, and represent perhaps the most promising tools for investigating protein lifetimes, transport, turnover rates and so on.

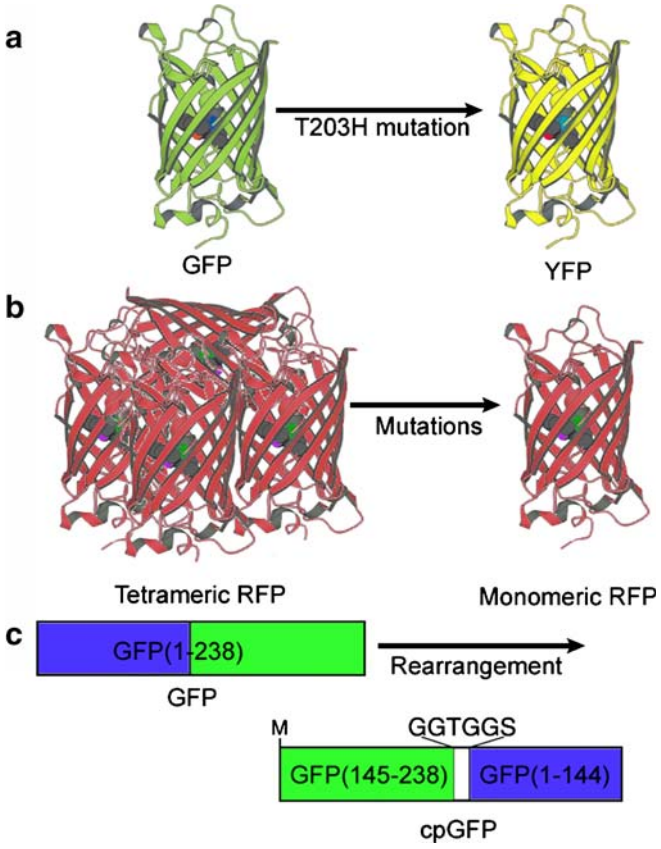

Fig. 2a–c Various FP mutants. **a** Introduction of the mutation of Thr203His in GFP results in significantly red-shifted maximum excitation and emission wavelengths; this mutant is named YFP. **b** By using mutagenesis, the original tetrameric DsRed is reconstructed into the monomeric DsRed variant. **c** Interchanging the amino and carboxyl portions of GFP and rejoining them with a short spacer generates cpGFP

Other kinds of fluorescent protein

Long-wavelength fluorescence can provide greater tissue penetration and better spectral separation from cellular autofluorescence. Therefore, red fluorescent proteins (RFP) are very useful in applications related to multicolor protein-tracking and the construction of sensors. The first RFP with a red emission wavelength was cloned from *Discosoma genus*, named "DsRed" [19]. Its structure is similar to GFP, but it is tetrameric. By using mutagenesis, different derivations exhibiting several advantages have been generated, such as the fluorescent timer of DsRed which has fluorescence that changes from green to red over time [20], the monomeric DsRed, named "mRFP1" [21] (Fig. 2b), as well as DsRed2 [22], T1 [23], and mCherry [24], which have chromophores that are brighter, more soluble, and mature faster than the original generation. Another orange-emitting fluorescent protein, which has higher pH-resistance and is more effective for imaging, was discovered in *Fungia concinn* [25]. In addition, "Kaede" [26], which is cloned from *Trachyphyllia geoffroyi*, can convert from green to red fluorescence and brightens 2,000-fold under UV illumination.

New rearrangement variants of fluorescent protein

In previous studies, fluorescent proteins were treated as an indivisible entity, usually appended to the amino or carboxyl terminus of the targeted protein. However, several rearrangements of GFPs in which the amino and carboxyl portions were interchanged and rejoined with a short spacer still remained fluorescent (Fig. 2c). These circular permutations exhibit several advantages, such as altered pK_a values, orientations of the chromophore with respect to a fusion partner, and greater absorbance of the exciting energy [27, 28].

Nongenetic fluorescent probes

However, there are some disadvantages of using FPs to perform OMI of the whole-body. Given the available wavelengths of excitation and emission and the power of the FP, optical imaging with a depth of penetration of approximately 1–2 mm limits their use to *C. elegans*, *Drosophila* or surface structures in small animals. To solve these problems, applying QDs (quantum dots) to OMI of

the whole-body could allow us to visualize biological events in deeper tissues with better image quality.

Compared with conventional organic dyes and fluorescent proteins, semiconductor nanocrystals—quantum dots—exhibit a narrow, tunable, symmetric emission spectrum and better photochemical stability. Also, their wavelengths of maximum excitation and emission shift to shorter wavelengths with decreasing size [29, 30]. QDs present several great advantages for whole-body OMI, such as their very large molar extinction coefficients and their very bright emission, which mean that the emission can be visualized in big animals [31]; the ability to perform simultaneous multiple color imaging of targets of interest [32]; and long excited state lifetimes that provide a way to separate the QD fluorescence from background fluorescence [33]. Because QDs are capped with a monolayer of organic ligands and are hydrophobic, they cannot be used for visualization in vivo. Goldman et al. [34] reported that QDs capped with fusion proteins of a specific antibody, protein G and leucine zipper adaptor protein could be used to image the target protein in vivo (Fig. 3). Since then, bioconjugated QDs have provided new approaches for the ultrasensitive and multiple-color imaging of targeted molecules in vivo. In addition, integrating QDs with paramagnetic substances results in new multimodality imaging probes that cuple the deep imaging capability of magnetic resonance imaging with ultrasensitive OMI [35]; these would be very powerful probes if used in clinical research. More recently, a new QD conjugate was found to emit long waves in the absence of external excitation light through bioluminous resonance energy transfer [36]. Compared with existing quantum dots, self-luminous quantum dots provide great sensitivity when imaging small animals, giving high signal-to-noise ratios.

OMI techniques

General imaging microscopy

Laser scanning confocal microscopy (LSCM) (Fig. 4a) and wide-field microscopy (WFM) are the tools most widely used for in vivo OMI. The major difference between them is that LSCM only collects the fluorescence emission of in-focus light, whereas WFM collects all signals, including out-of-focus light [37]. LSCM can produce superior images of multiple-cell samples, with photobleaching. However, LSCM cannot perform multiple-color imaging because it only observes in-focus light [38]. WFM is among the most sensitive of all such methods, permits minimal exposure of the sample, uniform illumination, an unlimited choice of excitation wavelengths, and is relatively simple [37]. One of the disadvantages of WFM is that disturbances are seen in observations of thicker specimens, where the out-of-focus signals become substantial [38].

Furthermore, multiple-photon laser scanning microscopy (MPLSM) has also been used in OMI [39]. The principle of MPLSM is that pulsed long excitation wavelength light, such as that provided by an infrared (IR) laser beam, is used to excite a molecule at the focal plane by multiple photons, causing fluorescence (Fig. 4b). The advantages of MPLSM are high tissue penetration ability (>30 μm), low photobleaching or photodamage, and a high signal/noise ratio (due to low autofluorescence) [40].

Second-harmonic imaging microscopy (SHIM)

SHIM is based on a nonlinear optical effect called second harmonic generation (SHG), commonly called frequency doubling. This phenomenon requires that intense laser light passes through a highly polarizable material with noncentrosymmetric molecular organization [41]. Biological macromolecules often assemble into large, ordered noncentrosymmetric structures and have highly polarizability. Therefore, high-resolution SHIM imaging can visualize living cells or tissues. This method provides several benefits: the targeted molecules are not excited, photobleaching does not occur, and it can detect information related to pathology. In addition, a combination of SHIM and MPLSM could make a powerful optical imaging technique.

Optical coherence tomography (OCT)

The principle of OCT imaging is analogous to that of ultrasound B-mode imaging, except that OCT uses light rather than acoustic waves [42]. OCT can provide cross-sectional imaging of structures below the tissue surface, analogous to histopathology. By using a state-of-the-art laser as the light source, ultrahigh-resolution imaging with axial resolutions as fine as 1–2 μm can be achieved [43].

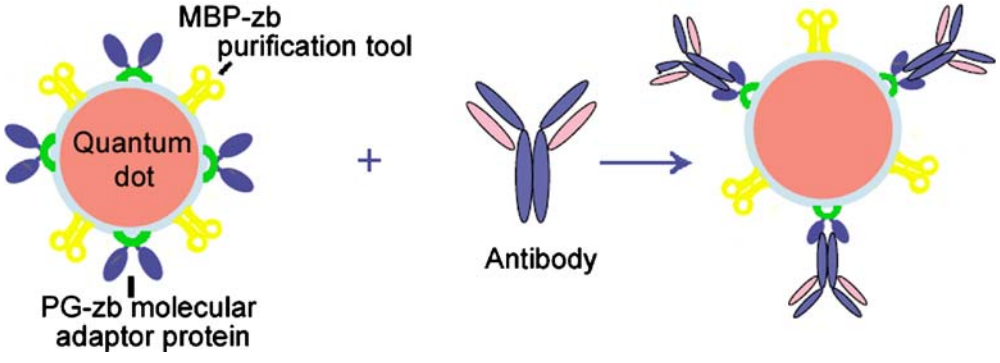

Fig. 3 Method of conjugating QDs to target proteins. The pG-zb acts as a molecular adaptor, connecting the QDs with the target protein through interactions of its protein G portion with a specific antibody as well as interactions of its positively charged tail with QDs capped with a negatively charged dihydrolipoic acid surface

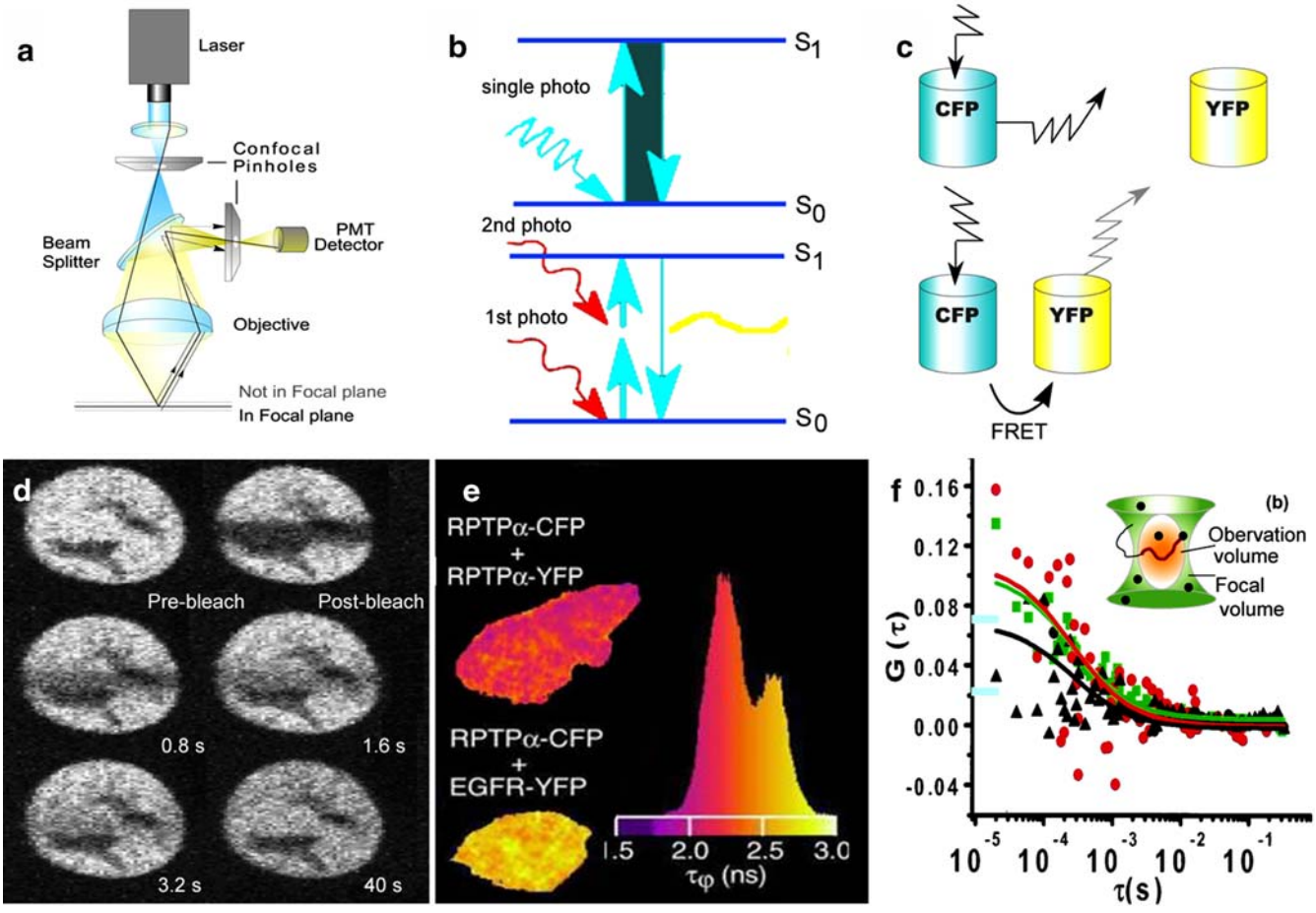

Fig. 4a–f Fluorescent OMI approaches. **a** LSCM only collects in-focus emitted light. **b** The principle of multiple photon excitation is based on the use of pulsed long excitation wavelengths to excite fluorescence. **c** FRET occurs between a donor and an acceptor that are in molecular proximity if the emission spectrum of the donor overlaps the excitation spectrum of the acceptor. **d** FRAP can reveal the mobility of FP-labeling proteins. These images illustrate the change in fluorescence of cells expressed with YFP-hGR before and after photobleaching. Reproduced from [51] with permission. **e** FLIM can measure the time-dependent emission intensity. The histogram represents the fluorescence lifetime distributions for the donor in the presence of interactions (*red*) or not (*yellow*). Reproduced from [57] with permission. **f** FCS can monitor the fluorescence signals emitted from the ROI. The cross-correlation curve (*black*) indicates a higher level of dimer or oligomer formation in the R1- and R5-expressing cells. Reproduced from [59] with permission

However, the penetration depth of the technique in most tissues is limited to approximately 2–3 mm [44]. Several features of OCT imaging make it well-suited to imaging-based diagnostics and surgical guidance, such as its high resolution, its ability to quantitatively assess, and its ability to image some tissue functions.

Fluorescent molecular imaging approaches

Fluorescence resonance energy transfer (FRET)

FRET is a quantum mechanical phenomenon that occurs between a fluorescence donor and a fluorescence acceptor with a favorable dipole–dipole orientation that are in molecular proximity to each other, provided the emission spectrum of the donor overlaps the excitation spectrum of the acceptor (Fig. 4c) [45]. Therefore, imaging based on FRET can determine the proximity (within the nanometer range) between labeled biomolecules in living cells [46, 47]. FRET-based microscopy includes intensity-based detection methods and fluorescence decay kinetics-based detection methods [46]. Similar to general fluorescence imaging microscopy, FRET also suffers from various drawbacks, like autofluorescence, detector noise, optical noise and photobleaching. In addition, spectral bleed-through (SBT), or cross-talk, is a major problem in FRET [48]. FRET is currently widely used in studies of protein colocalization, conformational changes, protein interactions and signal transduction [47, 49].

Fluorescence recovery after photobleaching (FRAP)

FRAP involves observing the rate of recovery of fluorescence resulting from the movement of a fluorescent marker into an area which contains the same marker that has been rendered nonfluorescent via an intense photobleaching pulse of laser light (Fig. 4d). FRAP has proved to be a powerful method for measuring the mobilities of target

molecules in various membranes, cytoplasms and nuclei [50]. For example, the mobility of the hormone receptor in the nucleus of a living cell [51], the mobility in subcellular compartments and the dynamics of vesicles inside the synapses of cultured hippocampal neurons [52] have been studied using this approach.

Fluorescence lifetime imaging microscopy (FLIM)

FLIM is a technique by which the mean fluorescence lifetime of a chromophore is measured at each spatially resolvable element of a microscope image [53]. The fluorescence lifetime is an inherent property of a chromophore that is sensitive to environmental and physical processes. Therefore, FLIM can detect interesting physical processes that can influence the excited state of a probe in vivo [54]. In addition, the mean lifetime of a donor is shifted to shorter lifetimes in the presence of an acceptor in FRET (Fig. 4e), so FLIM can detect changes in FRET [55], although this may not be valid in complex cellular systems that consist of several different lifetime components [56]. For example, using a FRET–FLIM method, the regulation of the activity of receptor protein tyrosine kinase (RPTK) through its dimerization was demonstrated in living cells [57]. The main drawbacks of FLIM are that it has relatively low sensitivity and requires expensive instrumentation.

Fluorescence correlation spectroscopy (FCS)

FCS is an approach that has emerged only recently. It is a high-sensitivity photon-counting technique that permits fluctuations in the fluorescence signal due to changes in the fluorescence quantum yield to be measured (Fig. 4f) [58]. Therefore, FCS can directly measure the mobilities of biomolecules, and it can monitor the average association and dissociation of target labeled with fluorescence probe—which vary with interaction kinetics, complex composition and complex size—in vivo without photobleaching. For example, FCS can be used to detect the clustering of somatostatin receptors [59] and the binding affinities of glucocorticoids (GC) in different subcellular compartments [60].

Applications of OMI

OMI for biomolecules

Originally, OMI of biomolecule function was performed on dead fixed cells or tissue sections in vitro. The first application of fluorescent detection in situ emerged in 1980, when RNA that was directly labeled with fluorophore was used as a probe for specific DNA sequences [61]. However, this method is not sensitive enough. Another indirect detection method allows signal to be significantly increased by binding secondary reporter to the hybridization probes that bind to targeted DNA [62] and mRNA [63]. Recently, Santangelo et al. [64] indicated that coinjection of two beacons based on FRET could be used to map the localization of a specific hybridization in living cells. Another application of FISH is immunocytochemistry (IC), which is used to detect target protein in specimens in vitro as antigen by means of antibodies labeled with fluorescence probe [65]. The technique of FISH is still being developed, with more specific fine-tuning of sensitivity and multiplicity necessary, after which its applications should gradually move from being in vitro to in vivo [66].

In addition, Fourier transform infrared (FT–IR) spectroscopy allows the simultaneous detection of nearly all organic molecules in a single spectrum and hence is ideally suited for the investigation of complex metabolic pathways. However, this advantage is only useful when powerful mathematical methods are available for the analysis of the highly complex spectra produced. Glycolytic intermediates In yeast extract were identified with FT–IR spectroscopy. The results were in good agreement with known phase relationships in oscillatory glycolysis [67]. In another experiment, glycogen, protein, lipid and nucleic acid concentrations were monitored in fish liver [68] using this method.

Single-molecule OMI is a very young field that holds great promise. It is not a technique, but a way of thinking that can allow us to detect individual molecular interactions, protein dynamics and signaling transduction pathways in living cells, which is difficult and sometimes impossible to achieve using conventional techniques [46]. For example, Sonnleitner et al. observed that the voltage-gated ion channel does not directly open or close under the conditions of single-molecular interaction using this approach [69]. Karymov et al. reported a method that could be used to directly follow junction branch migration in the holiday junction at the single-molecule level, and they detected that branch migration was a stepwise random process where the overall kinetics were dependent on the Mg^{2+} concentration [70].

Using OMI to monitor physiological processes in living cells

Monitoring gene expression and RNA localization

The fusion of gene promoter and fluorescent protein cDNA can be used to noninvasively analyze the expression pattern of a target gene, which is a very common approach used to study gene expression in vivo and is widely used in life science research. To minimize the accumulation of the background fluorescence that is generated by leaky, undegraded level (i.e. from previously expressed fluorescent protein that has not yet degraded), several chimeric EGFPs with shorter fluorescence half-lives were constructed by fusing protein [71, 72]. However, this approach leads to lower sensitivity, and cannot reveal low levels of expression. To overcome these drawbacks, a new approach that is similar to the amplification of an enzymatic reporter

was applied, which was then used in "enhancer-trap" strategies [73, 74]. The principle behind this is that the fluorescence of FP, revealing targeted gene expression in different tissues, is magnified through a transcript factor, which allows weak signals to be seen.

In addition, DNA and RNA sequences and other molecules could be visualized indirectly by labeling their binding proteins with FP in vivo. For example, by using RNA binding protein MS2 labeled with GFP, the mobility of targeted RNA could be visualized in vivo [75]. In another study, a similar method was used to observe gene expression correlated with a change in chromatin structure under the progress of transcription in real time [76]. Compared with FISH in vivo, the disadvantage of this method is the introduction of a protein complex of considerable size.

Monitoring protein and subcellular organelle dynamics

FP can also be used to monitor the behavior of the targeted protein, such as its appearance, degradation, localization, translocation and interaction in vivo. For example, by using a fusion protein of GR and FP, the dynamics of the exchange of GR with its binding sequence array can be monitored [77]. In addition, visualization of the dynamics of the GFP-GR fusion protein in vivo in more physiological conditions was achieved by using GFP-GR knock-in mice [78]. Another interesting application involves identifying the localization of an unknown protein on a large scale, a method termed the "protein trap," in which the imaging of cells containing the fusion protein of FP and a cDNA library was used to screen for target protein at the localization of interest [79].

Fusion protein that targets a given subcellular organelle is often used to study the dynamics of subcellular organelles. For example, Shaw et al. [80] revealed the dynamics of migration across the cell cortex of individual cortical microtubules in *Arabidopsis* by using tubulin fused to FP. In a similar study, this method was used to measure the rates of tubulin polymer growth, shortening and transition [81]. Furthermore, new subcellular structures can also be discovered by visualizing fusion FP, such as the novel discrete area in the nucleus, in which phytochrome species were induced to accumulated by light [82].

Monitoring general protein–protein interactions

Detecting the proximity of two biomolecules based on FRET is an approach widely used to observe protein interactions in real time in vivo. Most commonly, CFP and YFP are respectively fused to each of their putative interaction proteins, which are coexpressed in one living cell so that FRET between two fused FPs of interaction can be detected (Fig. 5a). A variety of protein interactions in different cells have been successfully visualized so far using intermolecular FRET, such as the interaction between

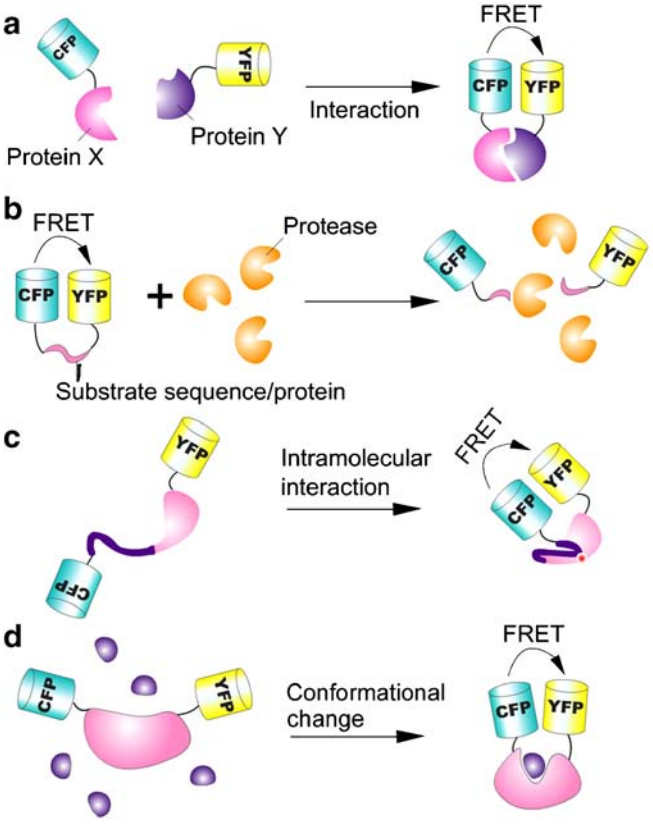

Fig. 5a–d General designs of FRET-based fluorescent probes. **a** An intermolecular probe consists of two interacting proteins that are labeled with CFP and YFP, respectively, which interact and result in FRET. **b** An intramolecular probe consists of CFP and YFP fused together with a cleavable linker or protein, which can be cleaved by proteolysis and disrupt FRET. **c** An intramolecular probe consists of sandwiching two domains between CFP and YFP, which can interact after phosphorylation or binding to calcium, resulting in a change in FRET. **d** An intramolecular probe consists of CFP, YFP and a protein/domain, which permits conformational change by binding to another biomolecule, leading to a change in FRET

phytochrome B and cryptochrome 2 [83], the rearrangement of G-protein subunits [84], and the oligomeric states of the ligands B7-1 and B7-2 [85]. Protein–protein interactions can also be imaged via protein complementation assays. The putative interaction proteins are respectively fused to two complementary fragments of one fluorescent protein, and then interaction of the proteins can reinvoke the fluorescence [46, 86], in a technique which is analogous to yeast two-hybrid assays (Fig. 6a). Using this method, Hu et al. simultaneously visualized several interactions among bZIP and Rel family transcription factors in one cell [87, 88].

Monitoring protease and kinase activity

The first reporter of proteolysis consists of BFP and GFP fusing together with a protease-sensitive linker, which exhibits the FRET phenomenon. Proteolysis can disrupt the FRET by separating the donor and acceptor fluorescent proteins [89]. In recent studies, fusion proteins of CFP,

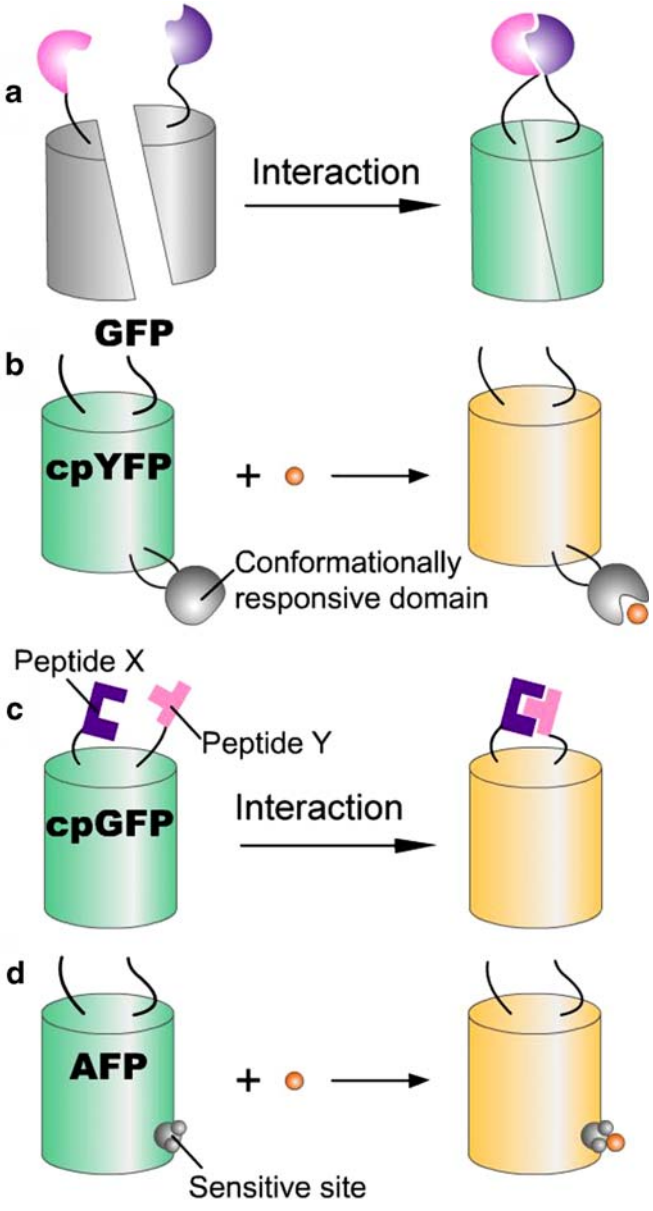

Fig. 6a–d Single FP-based fluorescent probes. **a** The probe consists of the fusion of two interacting proteins to two complementary fragments of one FP, respectively, which can interact and reinvoke the fluorescence. **b** Insertion of a conformationlly responsive domain/protein into cpYFP can lead to a change of fluorescence when its conformation is changed. **c** The probe consists of the fusion of two interacting proteins/domains to the amino and carboxyl termini of cpGFP, which can interact and change the cpGFP fluorescence. **d** By using mutagenesis, AFP can be engineered to be directly sensitive to a small molecule, such as Cl^-, H^+

YFP and a specific recognition sequence were used to measure the different caspase proteolytic activities during different apoptosis pathways (Fig. 5b) [90–92]. In another study, YFP-Bid-CFP fusion protein was used to visualize the activation of Bid protein by proteolytic cleavage, and translocation of the cleaved Bid to mitochondria was observed directly [93].

Reporters for the activity of tyrosine kinases and serine/threonine kinases have been made by sandwiching a substrate peptide for the kinase of interest and a phosphoaminoacid-binding domain, such as Src-homology-2 (SH2) or 14-3-3 protein, between two FPs (Fig. 5c). Phosphorylation of the substrate peptide induces the formation of an intramolecular complex with the phosphoaminoacid-binding domain, which leads to a change in the FRET. Meanwhile, these indicators also report the opposite phosphatase activity. This generic concept has so far been adapted to create probes for the phosphorylation of the kinase of interest in different signal transduction pathways, including phosphorylation of protein kinase A (PKA) [94], activation of serine/threonine kinase Akt [95], and activation of Src kinase on the cell membrane [96].

Monitoring changes in calcium

Genetically encoded fluorescent indicators for calcium without cofactors that can target to specific intracellular locations were first constructed by Miyawaki et al. [97]. This indicator was termed “cameleon.” The cameleon consists of the tandem fusion of CFP, calmodulin, the calmodulin-binding peptide M13 and YFP. Binding of Ca^{2+} allows calmodulin to wrap around the M13 domain, which increases the FRET between flanking FPs (Fig. 5c). Replacing YFP with cpYFP [28], Venus [98] or EYFP [99] led to a new generation of cameleon that exhibited better spatial and temporal resolution as well as better environmental resistance. In order to measure high concentrations of Ca^{2+}, the CaM–M13 interface of cameleon was re-engineered to reduce its affinity to Ca^{2+}, which improved the imaging of Ca^{2+} in the endoplasmic reticulum [100].

Other indicators for calcium that are not based on FRET have also been reported. cpGFP or cpYFP can tolerate the insertion of another entire protein, and conformational change of the fusion cpFP can change its fluorescence. Therefore, the insertion of calmodulin into cpYFP (called “camgaroos”) (Fig. 6b) [14, 27] and the tandem fusion protein of M13, cpGFP and calmodulin (termed “G-CaMP”) (Fig. 6c) [101] have both been used as calcium indicators because a conformational change occurs in the fusion cpFPs upon calcium binding.

Monitoring changes in cyclic nucleotides

The first fluorescent sensor of cAMP consists of cAMP-dependent protein kinase (PKA) in which the catalytic subunit and the regulatory subunit are labeled with a fluorescein and a rhodamine, respectively. Binding of cAMP to the labeled regulatory subunit leads to the dissociation of the labeled catalytic subunit, which disrupts the FRET between the two fluorescent dyes [102]. Later, this system was developed into a genetic cAMP indicator with BFP and GFP replacing the fluorescent dyes [103]. The most recent cAMP indicator was constructed by sandwiching a full length Epac1 between CFP and YFP (Fig. 5d) [104].

A genetically encoded indicator for another cyclic nucleotide, cGMP, has been reported by Sato et al. [105].

This indicator consists of a tandem fusion of BFP, nondimerizing mutants of cGMP-dependent protein kinase Iα (PKG Iα) and GFP. An increase in FRET between the two FPs can be detected upon the cGMP-induced conformational change of PKG Iα. Another sensor, termed "cygnet-1" [106], was constructed to have high selectivity for cGMP over cAMP. Here, the truncation of PKG Iα consisted of residues 1–77 rather than 1–47 reported in a previous study [105], and it exhibited decreased FRET fluorescence upon the binding of cGMP.

Monitoring changes in transmembrane voltage

Measuring electrical activity in living cells with high spatial and temporal resolution is a fundamental problem in studies of excited cell information processing. To address this problem, Siegel and Isacoff [107] first constructed a novel fluorescent probe that could be used to measure transmembrane voltage in vivo, termed the fluorescent shaker or "FlaSh", in which the modified GFP was inserted into a voltage-sensitive K^+ channel so that voltage-dependent rearrangements in the K^+ channel fusion protein could induce changes in the GFP fluorescence. A similar voltage sensor was generated by inserting GFP into another channel, the rat μI skeletal muscle voltage-gated Na^+ channel, and was named "SPARC" [108]. In other studies, Sakai et al. [109] developed a new voltage-sensitive indicator based on FRET, in which changes in membrane voltage can lead to changes in FRET.

Monitoring changes in pH in living cells

The chromophore of a FP is surrounded by a hydrogen-bonding network within the β-barrel, which means that the FP is pH-sensitive because of direct interactions between its hydrogen-bonding network and external protons [12]. The majority of GFP, YFP and their circularly permuted constructions described in previous parts of this review exhibit sensitivity to acid (Fig. 6d), whereas the original AFP—*Renilla reniformis* GFP—and DsRed are insensitive to acid. Therefore, acid-sensitive variants can serve as ideal donors in pH indicators based on FRET, and DsRed is the most desirable acceptor [110]. Another pH sensor has been generated by using a new group of pH-sensitive GFP variants, termed "deGFPs," which exhibit rapid changes in emission from green to blue as the pH decreases, and these are suitable for ratiometric measurements in vivo [111, 112].

Monitoring signal transduction from cell to cell

Scientists have also monitored intercellular changes in biomolecules and physiological events, which have been visualized in single cells in real time in a cell population. For example, Bedner et al. monitored the intercellular permeability to cAMP of six different gap junction channels by using sensors that are highly sensitive to cAMP concentration [113]. The change in calcium concentration from cell to cell was also monitored via calcium dyes [114]. In addition to these biomicromolecules, the propagation of intercellular apoptotic or survival events in monolayer cells mediated by the gap junction channel were also studied through OMI [115].

Using OMI to investigate tissue structure and function

It has recently been shown that SHIM can be used to directly detect several structural protein arrays in tissues, such as collagen arrays in mouse [116], neurons and muscular structures of the pharynx in *C. elegans* [117] without the need for fluorescent labeling. SHIM also readily retrieves more detailed molecular information than that obtained through the application of fluorescent labeling. Therefore, SHIM can be used to study or diagnose several diseases that are related to the assembly polarity of microtubule complexes in native brain tissue [118]. In addition, SHIM has proven to be crucial to neuroscience investigations in thick tissue preparations. For example, the fast neuronal membrane potential transient in mammalian brain slices labeled with FM4-64 dye was investigated by this method [119]. By labeling with another dye, the action potential was recorded with high temporal and spatial resolution on soma and neurite membranes [120].

OCT also has the ability to perform in situ, real-time imaging of tissue pathology, and it can be used to guide excisional biopsy in order to reduce false negatives caused by sampling errors. In particular, OCT enables the internal architectural morphology of the retina to be visualized noninvasively, and it can be used to diagnose and monitor retinal diseases, which cannot be achieved through any other methods [121]. The development of high-speed OCT imaging combined with small fiber-optic probes has enabled in vivo endoscopic imaging, such as the visualization of the oral cavity [122], the larynx and the bladder [123]. In addition, OCT can perform functional imaging of tissues, such as brain activity [124], inflammatory/neoplastic morphologic changes [125]. Raman spectroscopy (RS) is another powerful diagnostic tool that enables tissue identification and classification, as demonstrated by measurements of the brain tissue of a six-month-old pig by fiber-optic probes [126] and analysis of the molecular composition of human bronchial tissue structures [127]. Also, a combination of confocal RS and LSCM has been employed to obtain detailed information about the subsurface structures in the skin with high spatial resolution in a completely noninvasive manner [128].

OMI of organisms

Employing fluorescent protein

When performing whole-body OMI of organisms, the utilization of genetically encoded fluorescence probes has enabled scientists to decipher spatial and temporal changes

in biological events inside complex organisms [129]. Over the past few decades, FPs have been used to generate various fluorescent probes that have been used to image physiological and biochemical events in the monolayer cells. Extracting information from whole-body imaging is more relevant to real physiological conditions, but up to now, only a few fluorescent indicators have been used in complex organisms to visualize physiological activity in vivo.

To study the feeding behavior of *C. elegans*, Kerr et al. [130] introduced a calcium indicator based on cameleon to *C. elegans*, which allowed them to measure the Ca^{2+} signals evoked in pharyngeal muscles and individual neurons under the stimulation of feeding in vivo (Fig. 7a,b). Similar visualization of cameleon localized in other tissues was used to study the functions of serotonin and G proteins [131], the role of G proteins in signal transduction [132], and the ASH neuron response [133] in *C. elegans*. The

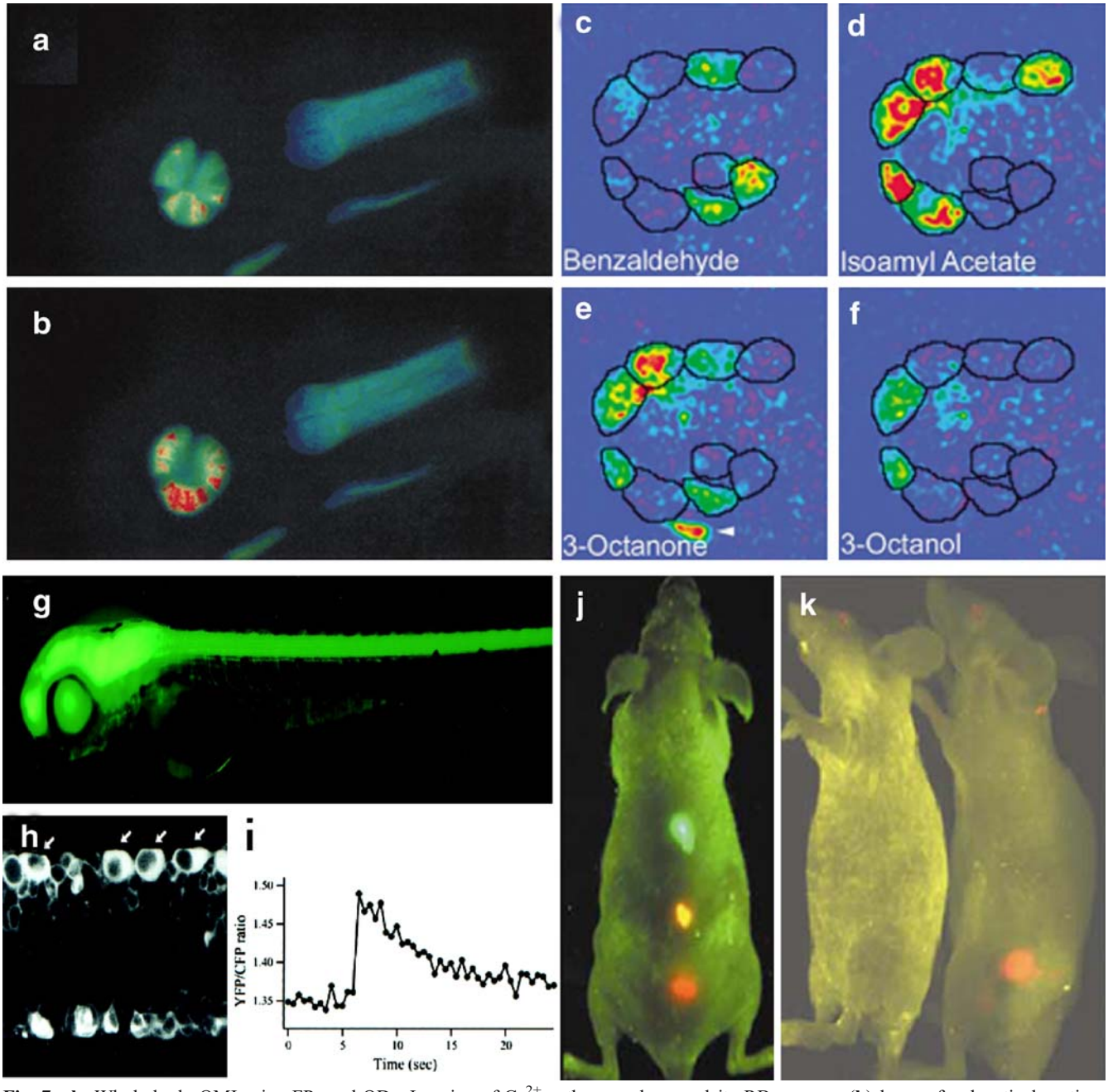

Fig. 7a–k Whole-body OMI using FPs and QDs. Imaging of Ca^{2+} signals in pharyngeal muscles under the conditions of noncontraction (**a**) and contraction (**b**) (*red color* indicates higher calcium) in transgenic *C. elegans* expressing cameleon. Reproduced from [130] with permission. **c**–**f** Ca^{2+} signals evoked by different odors in *Drosophila* brain expressing G-CaMP. Reproduced from [135] with permission. Imaging of a three-day-old transgenic fish (**g**) carrying the cameleon and its RB neurons (**h**) by confocal optical section, and the change in the fluorescence ratio (**i**) (representing the calcium concentration) in an RB neuron under electrical stimulation of the skin. Reproduced from [136] with permission. **j** Simultaneous multicolor imaging in a mouse injected with QD-encoded microbeads; **k** QD imaging of a prostate tumor in the mouse. Reproduced from [33] with permission

Table 1 OMI in systems biology

Techniques	Physical processes	Resolution	Sensitivity	Penetration	Observation methods	Probes	Indicator localization	References
WFM LSCM MPLSM	RNA transcription and expression	High	High	High	DFI, FRET	FPs	In vitro, cells, tissues, organism	[63, 64, 71–76]
	Protein localization and dynamics				DFI	FPs	In vitro, cells, tissues, organism	[51, 52, 65, 77–79]
	Subcellular organelle dynamics				DFI, FRAP	FPs	Cells	[80–82]
	Protein interaction				FRET, FLIM, FCS	FPs, cpFPs	Cells, mouse	[46, 47, 49, 57, 59, 60, 83–88, 140]
	Protease and kinase activity				FRET	FPs		[89–96]
	Calcium				DFI, FRET	FPs, cpFPs	Cells, *C. elegans*, fish, mouse, *Drosophila*	[14, 27, 28, 97–101, 130–138]
	cAMP, cGMP				FRET	FPs	Cells	[102–106]
	Electrical activity				DFI, FRET	FPs	Cells	[107–109]
	pH				DFI, FRET	FPs	Cells, mouse	[110–112, 139]
	Tumor				DFI	QDs	Mouse	[33, 141, 142]
SHIM	Biomacromolecules	Low	High	Low	NI	–	Mouse, *C. elegans*, brain tissue	[116–118]
	Membrane potential				NI	Dyes	Cells, brain tissue	[119, 120]
OCT	Morphology of tissue	High	Low	High	EI	–	Human	[122, 123]
	Activity and disease of organ				EI	–	Human	[124, 125]
RS	Composition of structure	Low	High	Low	NI	–	Brain tissues, bronchial tissue	[126, 127]
FT-IR	Kinetics of reaction intermediates	Low	High	Low	NI	–	Yeast extract, fish liver	[67, 68]

Abbreviations: *DFI*, Direct fluorescent imaging; *NI*, nonlinear imaging; *EI*, light-echo imaging

spatial and temporal representation of odorant-evoked Ca^{2+} signals in the *Drosophila* brain was explored using cameleon [134] and G-CaMP (Fig. 7c–f) [135]. Calcium imaging was also used in other animals, such as zebrafish (Fig. 7g–i) [136] and mouse [137, 138]. In addition, an indicator with pH sensitivity was used to visualize spatial patterns of defined neuronal activity in the mouse [139]. More recently, the proteolytic activity of calpain was visualized by introducing fluorescent indicator into living mouse muscle, which gave the first 3-D imaging of FRET in vivo [140].

Employing QDs

Due to several advantages of QDs over FP, QDs have been used to image large animals in vivo, which holds great promise for clinical applications, especially in the imaging of tumors. Akerman et al. [141] report the application of QDs coated with specific targeting peptides to the imaging of different tissues in tumor in vitro, but this QD probe cannot be detected in living animals. Gao et al. [33] report on a new class of multifunctional QDs that were encapsulated with an ABC triblock copolymer and then linked with a tumor-targeting antibody. Using subcutaneous injection or systemic injection of these QDs into the mouse, simultaneous multicolor fluorescence imaging of the prostate tumor with efficient background removal and precise delineation of weak spectral signatures based on wavelength resolution was achieved (Fig. 7j,k). More recent research showed that the utilization of QDs in combination with GFP labeling can differentiate tumor vessels from both perivascular cells and the matrix, and QDs linked to bone marrow-derived precursor cells can visualize tumor vasculature [142]. These OMI techniques, as well as their applications at different biological levels, are summarized in Table 1.

Future development

As described above, OMI is a feasible analytical technique for monitoring the dynamics of biological events in vivo and in real time anywhere from single-molecule to whole-body level, which makes it well-suited to systems biology measurements. Its noninvasive, ultrasensitive, high-resolution and real time nature has resulted in the widespread use of OMI. However, its disadvantages are also very apparent, such as its high cost, its low throughput, and its limited detectable depth, which is a particular hindrance in whole-body analysis. It should be pointed out that OMI is still far from fulfilling all of the requirements of systems biology (as concluded in our previous paper [8])—in terms of sensitivity, selectivity or specificity, linear range of quantitation, throughput, robustness, flexibility and cost—that are definitely required in genomics, transcriptomics, proteomics, and metabolomic profiling and dynamics, although it it clear that OMI is a promising method for these types of bioanalysis.

In the near future, several routes to improving OMI for systems biology need to be followed. Firstly, it is crucial to develop better molecular probes for OMI; in other words probes that have improved biocompatibilities and high quantum yields, are easy-to-tag, display multiple colors and have better penetration capabilities. The importance of the molecular probe to OMI cannot be overstressed. Current endeavors in QD development are heading in a good direction but this field is still in its infancy [143]. However, this doesn't mean that the development of small organic dyestuffs and biogenetic FP is less important: on the contrary, applications of these two kinds of molecular probes will still constitute most OMI studies [144]. Secondly, the integration of several modalities or approaches should be emphasized, since it makes OMI much more informative. Thirdly, efforts to improve OMI instrumentation are also important, since they will result in better time and space resolution and better sensitivity. For example, the 4Pi technique has improved the spatial resolution of OMI down to the mid-nanometer level, which is over the diffraction limit. The rapid progress currently being achieved in nanotechnology and nano/microelectromechanical systems looks set to lead to the manufacture of low-cost and high-efficiency OMI instruments [145]. Finally, the application of OMI to the life sciences is important; it is the reason behind the development of OMI. In particular, the application of OMI to systematic measurements of biological systems will be of great interest, which is also the aim of systems biology.

Acknowledgements The authors gratefully acknowledge financial support from the National Natural Science Foundation of China (Nos. 20405006, 30570468), the National High Technology Research and Development Program of China (863 Program: 2003AA231011), the Program for New Century Excellent Talents in University (NCET), and the Program for Distinguished Young Scientists of the Hubei Province (2004ABB004).

References

1. Kitano H (ed) (2001) Foundations of systems biology. MIT Press, Cambridge, MA
2. Liu ET (2005) Cell 121:505–506
3. Palsson B (2000) Nat Biotechnol 18:1147–1150
4. Hood L, Perlmutter RM (2004) Nat Biotechnol 22:1215–1217
5. Kitano H (2002) Science 295:1662–1664
6. Weiner N (1948) Cybernetics or control and communication in the animal and the machine. MIT Press, Cambridge, MA
7. Corttingham K (2005) Anal Chem 77:197A
8. Liu BF, Xu B, Zhang G, Du W, Luo Q (2006) J Chromatogr A 1106:19–29
9. Stephens DJ, Allan VJ (2003) Science 300:82–86
10. Farkas DL (2003) Nat Biotechnol 21:1269–1271
11. Farkas D (2003) Nat Biotechnol 21:1269–1271
12. Tsien RY (1998) Annu Rev Biochem 67:509–544
13. Ormo M, Cubitt AB, Kallio K, Gross LA, Tsien RY, Remington SJ (1996) Science 273:1392–1395
14. Griesbeck O, Baird GS, Campbell RE, Zacharias DA, Tsien RY (2001) J Biol Chem 276:29188–29194
15. Nagai T, Ibata K, Park ES, Kubota M, Mikoshiba K, Miyawaki A (2002) Nat Biotechnol 20:87–90
16. Rizzo MA, Springer GH, Granada B, Piston DW (2004) Nat Biotechnol 22:445–449

17. Sawano A, Miyawaki A (2000) Nucleic Acids Res 28:e78
18. Patterson GH, Lippincott-Schwartz J (2002) Science 297:1873–1877
19. Matz MV, Fradkov AF, Labas YA, Savitsky AP, Zaraisky AG, Markelov ML, Lukyanov SA (1999) Nat Biotechnol 17:969–973
20. Terskikh A, Fradkov A, Ermakova G, Zaraisky A, Tan P, Kajava AV, Zhao X, Lukyanov S, Matz M, Kim S, Weissman I, Siebert P (2000) Science 290:1585–1588
21. Campbell RE, Tour O, Palmer AE, Steinbach PA, Baird GS, Zacharias DA, Tsien RY (2002) Proc Natl Acad Sci USA 99:7877–7882
22. Terskikh AV, Fradkov AF, Zaraisky AG, Kajava AV, Angres B (2002) J Biol Chem 277:7633–7636
23. Bevis BJ, Glick BS (2002) Nat Biotechnol 20:83–87
24. Shaner NC, Campbell RE, Steinbach PA, Giepmans BN, Palmer AE, Tsien RY (2004) Nat Biotechnol 22:1567–1572
25. Karasawa S, Araki T, Nagai T, Mizuno H, Miyawaki A (2004) Biochem J 381:307–312
26. Ando R, Hama H, Yamamoto-Hino M, Mizuno H, Miyawaki A (2002) Proc Natl Acad Sci USA 99:12651–12656
27. Baird GS, Zacharias DA, Tsien RY (1999) Proc Natl Acad Sci USA 96:11241–11246
28. Nagai T, Yamada S, Tominaga T, Ichikawa M, Miyawaki A (2004) Proc Natl Acad Sci USA 101:10554–10559
29. Murray CB, Kagan CR, Bawendi MG (2000) Annu Rev Mater Sci 30:545–610
30. Green M, O'Brien P (1999) J Chem Soc Chem Commun 22:2235–2241
31. Leatherdale CA, Woo WK, Mikulec FV, Bawendi MG (2002) J Phys Chem B 106:7619–7622
32. Gao XH, Nie SM (2003) Trends Biotechnol 21:371–373
33. Jakobs S, Subramaniam V, Schonle A, Jovin TM, Hell SW (2000) FEBS Lett 479:131–135
34. Goldman ER, Anderson GP, Tran PT, Mattoussi H, Charles PT, Mauro JM (2002) Anal Chem 74:841–847
35. Wang DS, He JB, Rosenzweig N (2004) Nano Lett 4:409–413
36. So MK, Xu C, Loening AM, Gambhir SS, Rao J (2006) Nat Biotechnol 24:339–343
37. Gerlich D, Ellenberg J (2003) Nat Cell Biol Suppl S14–S19
38. Swedlow JR, Platani M (2002) Cell Struct Funct 27:335–341
39. Denk W, Strickler JH, Webb WW (1990) Science 248:73–76
40. Lansford R, Bearman G, Fraser SE (2001) J Biomed Opt 6:311–318
41. Campagnola PJ, Loew LM (2003) Nat Biotechnol 21:1356–1360
42. Fujimoto JG (2003) Nat Biotechnol 21:1361–1367
43. Drexler W, Morgner U, Kartner FX, Pitris C, Boppart SA, Li XD, Ippen EP, Fujimoto JG (1999) Opt Lett 24:1221–1223
44. Schmitt JM, Knüttel A, Yadlowsky M, Eckhaus MA (1994) Phys Med Biol 39:1705–1720
45. Sekar RB, Periasamy A (2003) J Cell Biol 160:629–633
46. Zhang J, Campbell RE, Ting AY, Tsien RY (2002) Nat Rev Mol Cell Biol 3:906–918
47. Miyawakib A (2003) Dev Cell 4:295–305
48. Berney C, Danuser G (2003) Biophys J 84:3992–4010
49. Herman B, Krishnan RV, Centonze VE (2004) Methods Mol Biol 261:351–370
50. Phair RD, Misteli T (2001) Nat Rev Mol Cell Biol 2:898–907
51. Schaaf MJ, Cidlowski JA (2003) Mol Cell Biol 23:1922–1934
52. Shtrahman M, Yeung C, Nauen DW, Bi GQ, Wu XL (2005) Biophys J 89:3615–3627
53. Bastiaens PI, Squire A (1999) Trends Cell Biol 9:48–52
54. Dong CY, French T, So PT, Buehler C, Berland KM, Gratton E (2003) Methods Cell Biol 72:431–464
55. Wouters FS, Verveer PJ, Bastiaens PI (2001) Trends Cell Biol 11:203–211
56. Subramaniam V, Hanley QS, Clayton AH, Jovin TM (2003) Methods Enzymol 360:178–201
57. Tertoolen LG, Blanchetot C, Jiang G, Overvoorde J, Gadella Jr TW, Hunter T, den Hertog J (2001) BMC Cell Biol 2:8
58. Berland KM (2004) Meth Mol Biol 261:383–398
59. Patel RC, Kumar U, Lamb DC, Eid JS, Rocheville M, Grant M, Rani A, Hazlett T, Patel SC, Gratton E, Patel YC (2002) Proc Natl Acad Sci USA 99:3294–3299
60. Maier C, Runzler D, Schindelar J, Grabner G, Waldhausl W, Kohler G, Luger A (2005) J Cell Sci 118:3353–3361
61. Bauman JG, Wiegant J, Borst P, van Duijn P (1980) Exp Cell Res 128:485–490
62. Manuelidis L, Langer-Safer PR, Ward DC (1982) J Cell Biol 95:619–625
63. Singer RH, Ward DC (1982) Proc Natl Acad Sci USA 79:7331–7335
64. Santangelo PJ, Nix B, Tsourkas A, Bao G (2004) Nucleic Acids Res 32:e57
65. Brandtzaeg P (1998) J Immunol Methods 216:49–67
66. Tanke HJ, Dirks RW, Raap T (2005) Curr Opin Biotech 16:49–54
67. Thomas M, LAAszlAA Z, Petro K, Andrea M, Stefan CM (2006) BioSystems 83:188–194
68. Cakmak G, Togan I, Severcan F (2006) Aquat Toxicol 77:53–63
69. Sonnleitner A, Mannuzzu LM, Terakawa S, Isacoff EY (2002) Proc Natl Acad Sci USA 99:12759–12764
70. Karymov M, Daniel D, Sankey OF, Lyubchenko YL (2005) Proc Natl Acad Sci USA 102:8186–8191
71. Li X, Zhao X, Fang Y, Jiang X, Duong T, Fan C, Huang CC, Kain SR (1998) J Biol Chem 273:34970–34975
72. Chiang CF, Okou DT, Griffin TB, Verret CR, Williams MN (2001) Arch Biochem Biophys 394:229–235
73. Phelps CB, Brand AH (1998) Methods 14:367–379
74. McGuire SE, Roman G, Davis RL (2004) Trends Genet 20:384–391
75. Bertrand E, Chartrand P, Schaefer M, Shenoy SM, Singer RH, Long RM (1998) Mol Cell 2:437–445
76. Janicki SM, Tsukamoto T, Salghetti SE, Tansey WP, Sachidanandam R, Prasanth KV, Ried T, Shav-Tal Y, Bertrand E, Singer RH, Spector DL (2004) Cell 116:683–698
77. Stavreva DA, Muller WG, Hager GL, Smith CL, McNally JG (2004) Mol Cell Biol 24:2682–2697
78. Usuku T, Nishi M, Morimoto M, Brewer JA, Muglia LJ, Sugimoto T, Kawata M (2005) Neuroscience 135:1119–1128
79. Gonzalez C, Bejarano LA (2000) Trends Cell Biol 10:162–165
80. Shaw SL, Kamyar R, Ehrhardt DW (2003) Science 300:1715–1718
81. Dhonukshe P, Gadella TW Jr (2003) Plant Cell 15:597–611
82. Kircher S, Gil P, Kozma-Bognar L, Fejes E, Speth V, Husselstein-Muller T, Bauer D, Adam E, Schafer E, Nagy F (2002) Plant Cell 14:1541–1555
83. Mas P, Devlin PF, Panda S, Kay SA (2000) Nature 408:207–211
84. Bunemann M, Frank M, Lohse MJ (2003) Proc Natl Acad Sci USA 100:16077–16082
85. Bhatia S, Edidin M, Almo SC, Nathenson SG (2005) Proc Natl Acad Sci USA 102:15569–15574
86. Michnick SW, Remy I, Campbell-Valois FX, Vallee-Belisle A, Pelletier JN (2000) Methods Enzymol 328:208–230
87. Hu CD, Chinenov Y, Kerppola TK (2002) Mol Cell 9:789–798
88. Hu CD, Kerppola TK (2003) Nat Biotechnol 21:539–545
89. Heim R, Tsien RY (1996) Curr Biol 6:178–182
90. Suzuki M, Ito Y, Sakata I, Sakai T, Husimi Y, Douglas KT (2005) Biochem Biophys Res Commun 330:454–460
91. Mahajan NP, Harrison-Shostak DC, Michaux J, Herman B (1999) Chem Biol 6:401–409
92. Rehm M, Dussmann H, Janicke RU, Tavare JM, Kogel D, Prehn JH (2002) J Biol Chem 277:24506–24514
93. Onuki R, Nagasaki A, Kawasaki H, Baba T, Uyeda TQ, Taira K (2002) Proc Natl Acad Sci USA 99:14716–14721
94. Zhang J, Ma Y, Taylor SS, Tsien RY (2001) Proc Natl Acad Sci USA 98:14997–15002
95. Ananthanarayanan B, Ni Q, Zhang J (2005) Proc Natl Acad Sci USA 102:15081–15086
96. Wang Y, Botvinick EL, Zhao Y, Berns MW, Usami S, Tsien RY, Chien S (2005) Nature 434:1040–1045

97. Miyawaki A, Llopis J, Heim R, McCaffery JM, Adams JA, Ikura M, Tsien RY (1997) Nature 388:882–887
98. Evanko DS, Haydon PG (2005) Cell Calcium 37:341–348
99. Truong K, Sawano A, Mizuno H, Hama H, Tong KI, Mal TK, Miyawaki A, Ikura M (2001) Nat Struct Biol 8:1069–1073
100. Palmer AE, Jin C, Red JC, Tsien RY (2004) Proc Natl Acad Sci USA 101:17404–17409
101. Nakai J, Ohkura M, Imoto K (2001) Nat Biotechnol 19:137–141
102. Adams SR, Harootunian AT, Buechler YJ, Taylor SS, Tsien RY (1991) Nature 349:694–697
103. Zaccolo M, Pozzan T (2002) Science 295:1711–1715
104. Dipilato LM, Cheng XD, Zhang J (2004) Proc Natl Acad Sci USA 101:16513–16518
105. Sato M, Hida N, Ozawa T, Umezawa Y (2000) Anal Chem 72:5918–5924
106. Honda A, Adams SR, Sawyer CL, Lev-Ram V, Tsien RY, Dostmann WR (2001) Proc Natl Acad Sci USA 98:2437–2442
107. Siegel MS, Isacoff EY (1997) Neuron 19:735–741
108. Ataka K, Pieribone VA (2002) Biophys J 82:509–516
109. Sakai R, Repunte-Canonigo V, Raj CD, Knopfel T (2001) Eur J Neurosci 13:2314–2318
110. Miyawaki A, Mizuno H, Nagai T, Sawano A (2003) Methods Enzymol 360:202–225
111. Hanson GT, McAnaney TB, Park ES, Rendell ME, Yarbrough DK, Chu S, Xi L, Boxer SG, Montrose MH, Remington SJ (2002) Biochemistry 41:15477–15488
112. McAnaney TB, Park ES, Hanson GT, Remington SJ, Boxer SG (2002) Biochemistry 41:15489–15494
113. Bedner P, Niessen H, Odermatt B, Kretz M, Willecke K, Harz H (2006) J Biol Chem 281:6673–6681
114. Dakin K, Zhao Y, Li WH (2005) Nat Methods 2:55–62
115. Nodin C, Nilsson M, Blomstrand F (2005) J Neurochem 94:1111–1123
116. Lyubovitsky JG, Spencer JA, Krasieva TB, Andersen B, Tromberg BJ (2006) J Biomed Opt 11:14013
117. Filippidis G, Kouloumentas C, Voglis G, Zacharopoulou F, Papazoglou TG, Tavernarakis N (2005) J Biomed Opt 10:024015
118. Dombeck DA, Sacconi L, Blanchard-Desce M, Webb WW (2005) J Neurophysiol 94:3628–3636
119. Nuriya M, Jiang J, Nemet B, Eisenthal KB, Yuste R (2006) Proc Natl Acad Sci USA 103:786–790
120. Dombeck DA, Blanchard-Desce M, Webb WW (2004) J Neurosci 24:999–1003
121. van Velthoven ME, Verbraak FD, Yannuzzi LA, Rosen RB, Podoleanu AG, de Smet MD (2006) Retina 26:129–136
122. Feldchtein FI, Gelikonov GV, Gelikonov VM, Iksanov RR, Kuranov RV, Sergeev AM, Gladkova ND, Ourutina MN, Warren Jr JA, Reitze DH (1998) Opt Express 3:239–250
123. Zagaynova EV, Streltsova OS, Gladkova ND, Snopova LB, Gelikonov GV, Feldchtein FI, Morozov AN (2002) J Urol 167:1492–1496
124. Maheswari RU, Takaoka H, Kadono H, Homma R, Tanifuji M (2003) J Neurosci Meth 124:83–92
125. Whiteman SC, Yang Y, van Pittius DG, Stephens M, Parmer J, Spiteri MA (2006) Clin Cancer Res 12:813–818
126. Santos LF, Wolthuis R, Koljenovic S, Almeida RM, Puppels GJ (2005) Anal Chem 77:6747–6752
127. Koljenovic S, Bakker Schut TC, van Meerbeeck JP, Maat AP, Burgers SA, Zondervan PE, Kros JM, Puppels GJ (2004) J Biomed Opt 9:1187–1197
128. Caspers PJ, Lucassen GW, Puppels GJ (2003) Biophys J 85:572–580
129. Miyawaki A (2003) Curr Opin Neurobiol 13:591–596
130. Kerr R, Lev-Ram V, Baird G, Vincent P, Tsien RY, Schafer WR (2000) Neuron 26:583–594
131. Shyn SI, Kerr R, Schafer WR (2003) Curr Biol 13:1910–1915
132. Fukuto HS, Ferkey DM, Apicella AJ, Lans H, Sharmeen T, Chen W, Lefkowitz RJ, Jansen G, Schafer WR, Hart AC (2004) Neuron 42:581–593
133. Hilliard MA, Apicella AJ, Kerr R, Suzuki H, Bazzicalupo P, Schafer WR (2005) EMBO J 24:63–72
134. Fiala A, Spall T, Diegelmann S, Eisermann B, Sachse S, Devaud JM, Buchner E, Galizia CG (2002) Curr Biol 12:1877–1884
135. Wang JW, Wong AM, Flores J, Vosshall LB, Axel R (2003) Cell 112:271–282
136. Higashijima S, Masino MA, Mandel G, Fetcho JR (2003) J Neurophysiol 90:3986–3997
137. Nyqvist D, Mattsson G, Kohler M, Lev-Ram V, Andersson A, Carlsson PO, Nordin A, Berggren PO, Jansson L (2005) J Endocrinol 186:333–341
138. Hara M, Bindokas V, Lopez JP, Kaihara K, Landa LR Jr, Harbeck M, Roe MW (2004) Am J Physiol Cell Physiol 287: C932–C938
139. Metzger F, Repunte-Canonigo V, Matsushita S, Akemann W, Diez-Garcia J, Ho CS, Iwasato T, Grandes P, Itohara S, Joho RH, Knopfel T (2002) Eur J Neurosci 15:40–50
140. Stockholm D, Bartoli M, Sillon G, Bourg N, Davoust J, Richard I (2005) J Mol Biol 346:215–222
141. Akerman ME, Chan WCW, Laakkonen P, Bhatia SN, Ruoslahti E (2002) Proc Natl Acad Sci USA 99:12617–12621
142. Stroh M, Zimmer JP, Duda DG, Levchenko TS, Cohen KS, Brown EB, Scadden DT, Torchilin VP, Bawendi MG, Fukumura D, Jain RK (2005) Nat Med 11:678–682
143. Seydel C (2003) Science 300:80–81
144. Lippincott-Schwartz J, Patterson GH (2003) Science 300: 87–91
145. Hell SW (2003) Nat Biotechnol 21:1347–1355